

32nd ASC Technical Conference, 2017

Topic: *Damage and Failure Prediction*

Keywords: Progressive failure, meso-scale, composites

Three-Dimensional High Fidelity Progressive Failure Damage Modeling of NCF Composites

**Venkat Aitharaju^{1*}, Satvir Aashat², Hamid G. Kia¹ Arunkumar Satyanarayana³,
Philip B. Bogert³**

¹General Motors Global Research and Development, Warren, MI, 48092

²Engineering Technology Associates, Troy, MI 48083, U.S.A.

³NASA Langley Research Center, Hampton, VA 23681, U.S.A.

*Corresponding Author: Venkat.aitharaju@gm.com

Abstract

Performance prediction of off-axis laminates is of significant interest in designing composite structures for energy absorption. Phenomenological models available in most of the commercial programs, where the fiber and resin properties are smeared, are very efficient for large scale structural analysis, but lack the ability to model the complex nonlinear behavior of the resin and fail to capture the complex load transfer mechanisms between the fiber and the resin matrix. On the other hand, high fidelity meso-scale models, where the fiber tows and matrix regions are explicitly modeled, have the ability to account for the complex behavior in each of the constituents of the composite. However, creating a finite element model of a larger scale composite component could be very time consuming and computationally very expensive. In the present study, a three-dimensional meso-scale model of non-crimp composite laminates was developed for various laminate schemes. The resin material was modeled as an elastic-plastic material with nonlinear hardening. The fiber tows were modeled with an orthotropic material model with brittle failure. In parallel, new stress based failure criteria combined with several damage evolution laws for matrix stresses were proposed for a phenomenological model. The results from both the meso-scale and phenomenological models were compared with the experiments for a variety of off-axis laminates.

Introduction

Carbon fiber composites are slowly entering the automotive design space due to their exceptional mechanical properties such as specific stiffness, specific strength and tailorability. They also have huge potential to achieve significant parts consolidation in safety critical automotive assemblies due to the ability to manufacture complex geometries. Fiber reinforced composites can offer designers a wider choice of selection with respect to fibers, resins, lay-up and thickness. It is costly and time consuming to arrive at an optimum lay-up to meet the specific performance if research is approached with experiments alone. Availability of a predictive tool for composite performance is essential to eliminate the trial and error, saving time and cost. However, composites present several challenges when it comes to predicting performance due to the complex failure modes that occur at various length scales and that often interact with each other. The main failure modes for composites are matrix compression, matrix tension, fiber compression, fiber tension, and delamination between the plies. The failure modes involving the fiber and matrix are termed as intra-laminar failures and delamination between the plies is termed as inter-layer failure. Figure 1 shows several possible analysis length-scales for the composite. The individual fiber-resin length-scale operates at a very small length scale of a few micro meters and the analysis models become computationally prohibitive for any practical analysis even at a small coupon level. However, the fiber tows comprised of thousands of fiber filaments operate in a length scale of 2-4 mm and simulation problems are solvable, thanks to the recent availability of high performance computational resources. The next length scale operates at the lamina level where the fiber and matrix are homogenized. This has been a traditional area of study. Several failure criteria were proposed to predict the failures at the constituent level based on the stresses evaluated at the lamina level. Hashin and Rotem [1], Hashin [2], Davila [3] and Pinho [4] developed various models to predict the initiation of the failure at the lamina level in each of the constituents. Subsequent to the initiation of the failure, the stiffness and strength properties of the lamina are degraded systematically. Many of the proposed failure models operating at the lamina level are somewhat reliable in predicting brittle failures, but still face some challenges in predicting ductile modes. The ductile modes of failure of the composite involve progressive failure of the matrix involving matrix yielding, plasticity, and finally scissoring of the fibers.

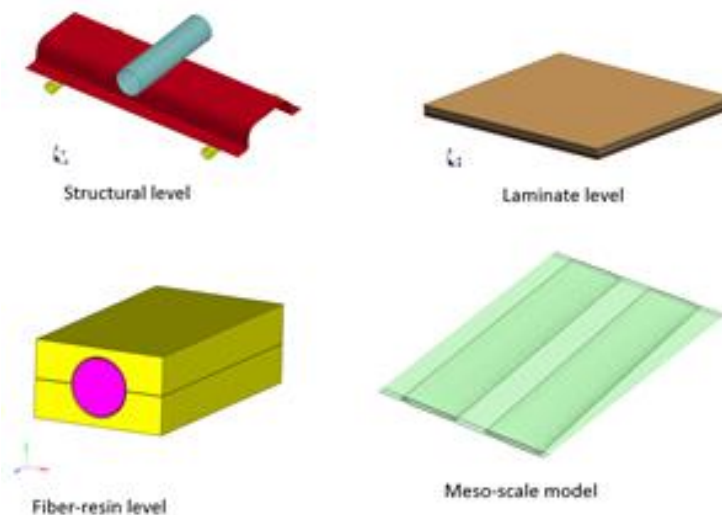


Figure 1: Length scales of the composite for analysis

Phillips et.al [5] developed a meso-scale model accounting for intra-laminar and inter-layer failures to study damage development in angle-ply coupons and a composite panel with a terminated stiffener. They showed that as the fiber orientation changes from 10 to 45°, the mode of failure changes from inter-layer damage to intra-layer damage, consistent with experimental observations. Hirsekorn et.al [6] studied the mechanical behavior of textile composites modeled at meso-scale, taking into account the influence of dry fabric preforming. Damage in the meso-scale model was introduced into the FE model by inserting transverse yarn cracks and micro-decohesion at the yarn surfaces around the crack tips. Even though the crack geometry was simplified, the results were encouraging.

High stiffness and high strength have been the major driver in designing components in the aerospace industry to meet the damage tolerant performance requirements without causing any failure in the service life. In contrast, the automotive industry is forced to design the structural components of the automobile to meet crash loading for which energy absorption is very important. During the crash loading, the structural composite may undergo complete failure and it is very important to predict the behavior during and after the failure to design components optimally. Many times, designing the laminates to behave in a ductile fashion during the loading will allow them to absorb more energy than the conventional brittle composites.

In the present study, first a meso-scale model was developed to model the progressive failure in the composite. Next, the progressive failure analysis model developed previously by the authors [7,8] was extended to include nonlinear shear behavior. Both the models were first calibrated to a particular off-axis lay-up and then further validated against experiments for other laminate schemes. The sections below provide the details of the material system chosen for the study, development of meso-scale and phenomenological models, comparison of experimental results with numerical results, and are followed by conclusions.

Material Description – Samples for Experiments

Non-crimp fabric (NCF) carbon fiber material procured from Sigmatech was used in the present study. The NCF preform has the nomenclature Sigmatech BMC933 1270mm-50” / T700SC 50K product # MC9331270. Four layers of such fabric was used to mold angle ply laminates with orientation sequence (θ /- θ /- θ /0). Several plaques with 30°, 45°, 60° angle ply laminates were molded at General Motors Research Laboratories using squeeze molding. The resin used in the RTM system was Hexion EPIKOTE epoxy resin with trade name TRAC 06170. The curing agent was EPIKURE with trade name TRAC 06170. The mold temperature was kept at 90 °C to inhibit curing before the start of compression of the mold. Square geometry plaques with size 444.5 mm x 444.5 mm and a thickness of 2.8 mm were molded. From the molded plaques, standard coupons were cut to conduct the tensile experiments.

Meso-Scale Models:

For the meso-scale model, fiber tows and matrix outside of the tows were discretized separately using three dimensional finite elements. The tow behavior was modeled using a progressive failure model available in the LS-DYNA computer program (material model # 54). The matrix behavior was modeled using an elastic-plastic material (material model # 24) with strain rate.

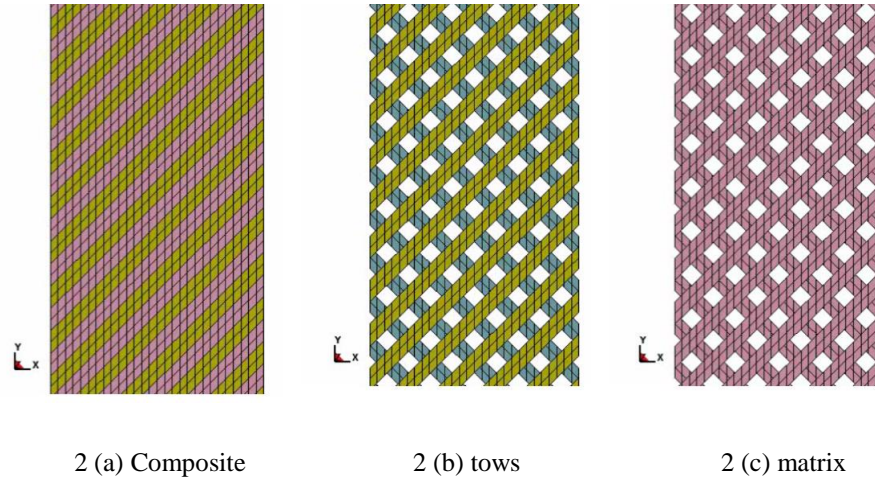


Figure 2. Meso-scale model for the (45/-45) composite

Table 1: Mechanical properties of the tow and resin used in the study.

Mechanical Property	Longitudinal Modulus (GPa)	Transverse Modulus (GPa)	Shear Modulus (GPa)	Poisson's Ratio	Tensile Strength (GPa)	Transverse Strength (GPa)
Tow (orthotropic)	230	20	8	0.3	2.63	.300
Matrix (isotropic)	5	-	-	0.3	.090	-

Figure 2 (a) shows finite element models for tow and matrix in a single layer of 45^0 degree angle ply. The model for the tows in the 45/-45 lay-up is shown in Figure 2 (b) and each ply of tows was modeled with an orthotropic material and a Chang- Chang failure criteria applied. The matrix is shown in Figure 2(c). A cohesive model based on a traction-separation law was used to model the inter-layer damage (delamination) between the layers. Table 1 shows the properties of the stiffness and strength used for modeling the tow and resin, respectively. These meso-scale models were used to model the behavior of several off-axis layups and the predictions were compared with the experimental results. In the analysis procedure, the 45/-45 lay-up was used to calibrate the elastoplastic behavior of the resin. Further, the results for the 30/-30 and 60/-60 lay-up were used for the laminate validation.

Phenomenological Damage Model

Even though meso-scale models have the ability to predict crack paths accurately in the off-axis plies, construction of such model for a composite laminate with off-axis plies is tedious and time consuming. Many continuum damage models predict the crack path more accurately in cross plies ($0^0/90^0$) than in off-axis plies ($+0^0/-0^0$) for laminates when the element edges are aligned along 0^0

and 90° ply orientations. The influence of element edge orientation along the fiber direction on the prediction of crack path is demonstrated in ref [9]. In the current work, a previously developed in-plane damage model [7, 8] was extended by including nonlinear shear stress strain behavior. This allowed the accurate prediction of crack path for the case with the element edges not aligned along the fiber directions.

Shear Stiffness Degradation Methodology

The original phenomenological model [8] degrades the transverse and shear stresses to zero instantaneously when the matrix fails either due to transverse or shear stresses reaching the failure limit as shown in Figure 3. This approach may cause improper load distribution in the element due to the sudden loss of shear and transverse stiffness especially in off-axis plies. Hence in the present approach where the fibers are not parallel to the loading direction, the transverse stress is reduced to zero instantaneously, but the shear stress is reduced by the matrix volume fraction and allowed to reach the max shear strength limit as shown in Figure 4.

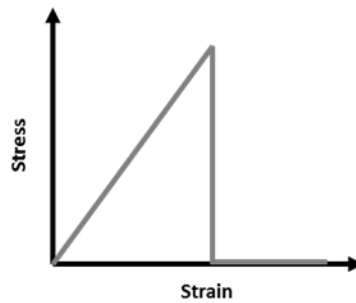


Figure 3. Transverse and Shear Stress Degradation law of original COSTR damage model.

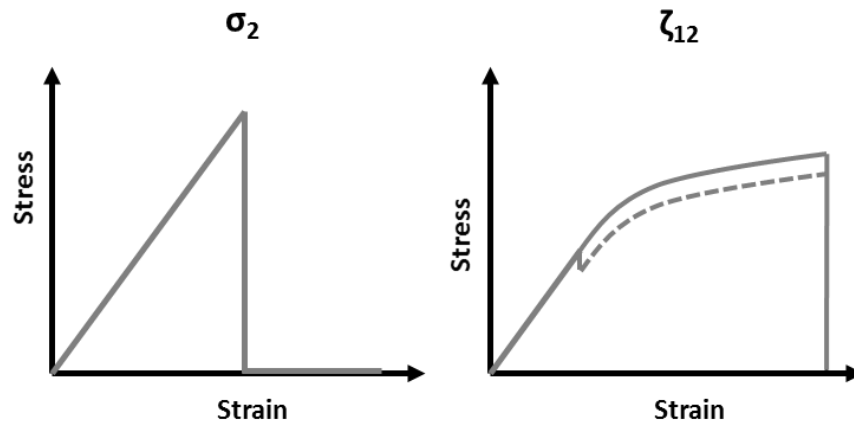
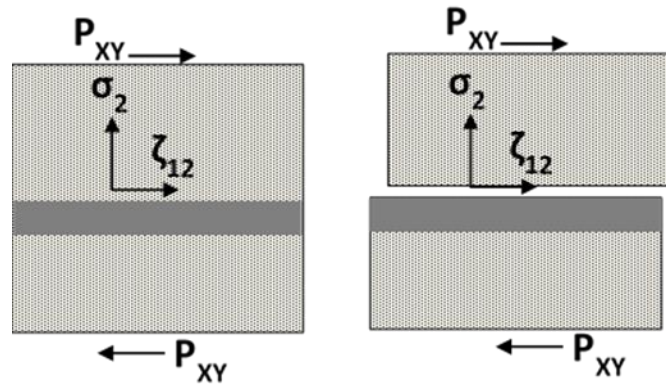
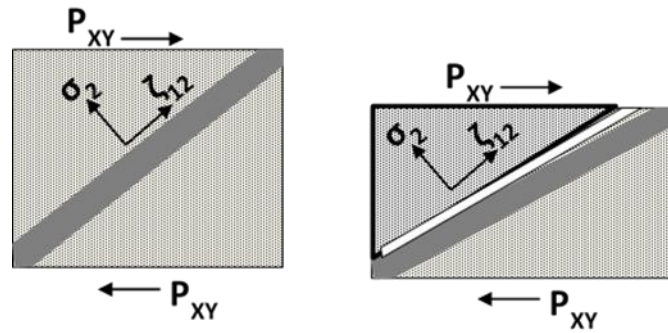


Figure 4. Transverse and Shear Stress Degradation law of modified damage model.

The hypothesis for degrading the shear stress in an element as shown in Figure 4 is explained in Figure 5.



a. Load P_{XY} Parallel to Fiber



b. Load P_{XY} Inclined to Fiber (Off-axis Plies)

Figure 5. : Hypothesis for Shear Stiffness Degradation Approach.

Figure 5 (a) shows the element with fibers aligned in the direction X subjected to a shear load P_{XY} . When the element fails due to the shear stress reaching the strength limit, the fibers do not offer any stiffness in the shear direction. For this reason, the shear stress is reduced to zero instantaneously in the plies. In the Figure 5 (b), the situation with fibers aligned oblique to the shear loading in an element is shown. One can visualize that after the shear stresses reaches the strength limit, fibers can still offer some resistance to shear deformation. To model this behavior, the shear stiffness is reduced by the matrix volume fraction (V_m) of the lamina. This reasoning is currently applied to uni-axial loading but may be easily modified and verified later for multi-axial loading.

Another modification made to the damage model is in the matrix damage detection criterion. Along with the Hashin-Rotem failure criterion for the matrix material, the strain in the fiber direction

should be positive under tension and negative under compression for a material point to be considered as damaged.

Finite Element Analysis (Meso-scale and phenomenological models)

The sample coupon considered for testing is 254 mm long and 25.4 mm wide. The tensile coupon was held using the loading grips for a distance of 50 mm from each end. The thickness of the sample is around 2.8 mm. Three different off-axis lay-ups were considered for the study. The numerical results from the meso-scale model and improved phenomenological model were compared with experimental results.

The tensile sample used in the experiments was modeled using 3-D solid finite elements. In the meso-scale model, three dimensional solid elements were used to discretize the tows and the matrix separately. Each layer was modeled with one solid element in the thickness direction. One point integration solid elements with hourglass correction were used for computational efficiency. The nodes belonging the tows and matrix are made coincident at the interfaces. A cohesive traction-separation law was used to model the delamination failure. The meso-scale analysis was performed using the LS-DYNA computer program. In the phenomenological model, the thickness of the sample was discretized with three homogenized sub-laminates with the cohesive layer modeled between them to simulate the delamination failure. The entire stacking sequence with cohesive layers for the three laminates is [30/coh/-30/-30/coh/30], [45/coh/-45/-45/coh/45] and [60/coh/-60/-60/coh/60]. No cohesive layers were used between the plies with the same orientation. Each of the sub-laminate layers is discretized using Abaqus continuum shell eight node reduced order integration elements (SC8R) with element size of 1.27 mm by 1.27 mm. The cohesive layers were modeled with COH3D8 type elements with zero thickness with a mesh size of 0.5 mm x 0.5 mm in the in-plane direction of the laminate. The sub-laminate layers and cohesive surfaces were connected using tie constraints. In both models the elements in the area of the stationary grips were constrained in all degrees of freedom. The elements under the moving grip was constrained in all the directions except the loading direction. A uniform velocity was prescribed. The velocity used in the simulation was scaled to obtain the results in a reasonable time without losing any accuracy (kinetic energy of the system was kept lower than 5% of the total energy). The finite element model of a typical laminate for the meso-scale model and phenomenological model are shown in Figure 6.

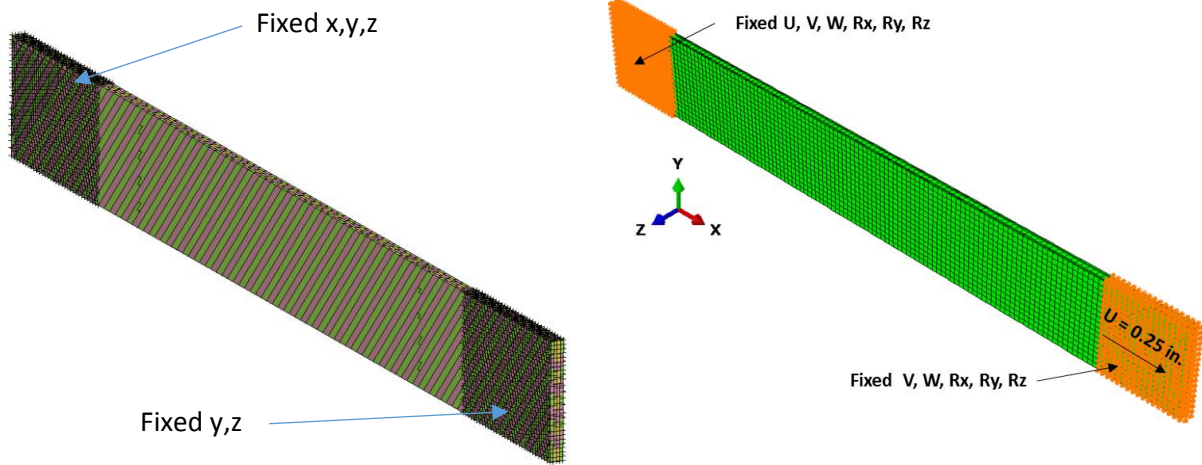


Figure 6. Finite Element Mesh of meso-scale and phenomenological model

Table 2: Mechanical properties of the uni-directional lamina used for phenomenological model

Properties	Values
E_1 (GPa)	137.90
E_2 (GPa)	6.21
G_{12} (GPa)	3.20
ν_{ue12}	0.35
X_T (GPa)	1.40
X_C (GPa)	0.74
Y_T (GPa)	0.026
Y_C (GPa)	0.169
S_{XY} (GPa)	0.045
G_{Ic} (J/m ²)	1059.5
G_{IIc}, G_{IIIc} (J/m ²)	2189.07

The properties and strengths of the composite ply and the cohesive layer are listed in Table 2. Even though a shear modulus was provided in the table, nonlinear shear stress versus strain data obtained from the experiments was used in the analysis.

Tensile loading [45/-45/-45/45] Laminate:

Figure 7 shows the shear stress and strain behavior of the resin system which was extracted from the tensile test of the 45° laminate. This curve was used as an input to the model. The failure strain for shear was assumed to 2.55%. In Figure 8, the load versus axial strain results of the laminate in tension is presented for both the phenomenological and meso-scale models. One can see a good correlation of failure load and slope of the curve when comparing the simulations and the experimental results.

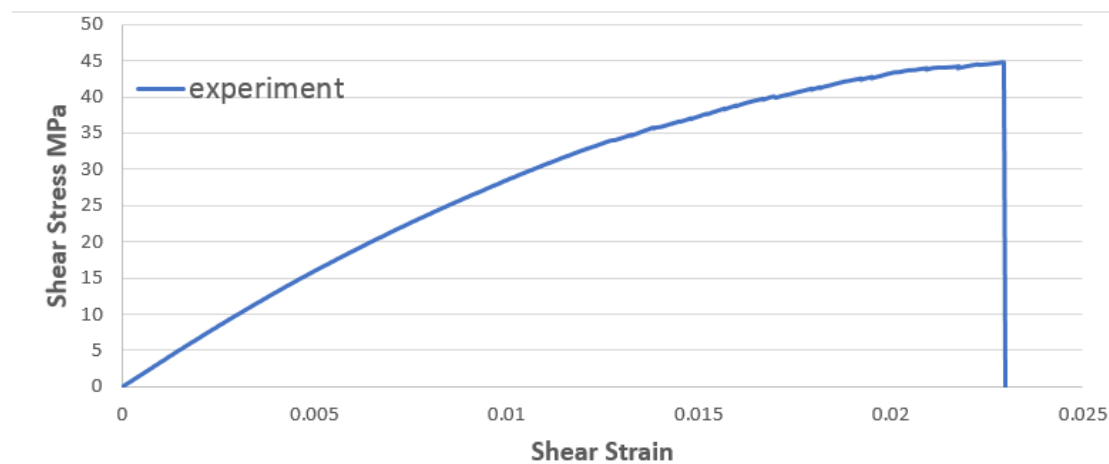


Figure 7. Shear stress vs shear strain curve from experimental tensile test.

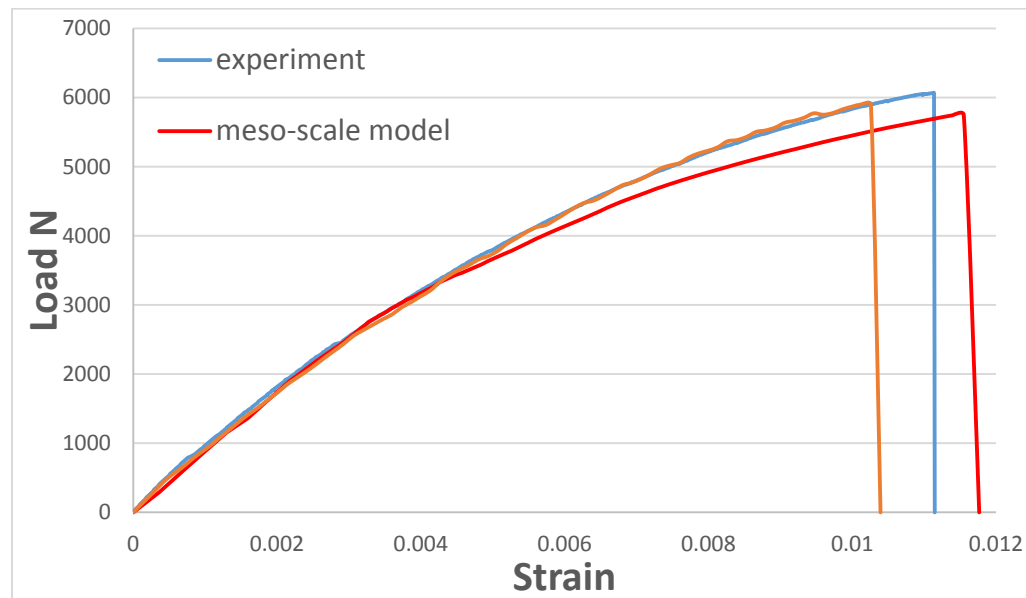


Figure 8: Load vs. Axial Strain of a [45/-45/-45/45] laminate coupon

Failure paths in sub-laminate layers from both meso-scale (tows and matrix) and phenomenological models are presented in Figure 9. Delaminations at the interfaces are presented in Figure 10 from the phenomenological model. Even though the sub-laminate layers fail mainly due to the in-plane shear stress reaching the failure limit, when the quadratic combination of these strains (transverse and shear) reaches a failure strain of 0.075 microns, the element is removed to simulate the crack formation. Hence in this simulation, no elements were deleted due to fiber failure.

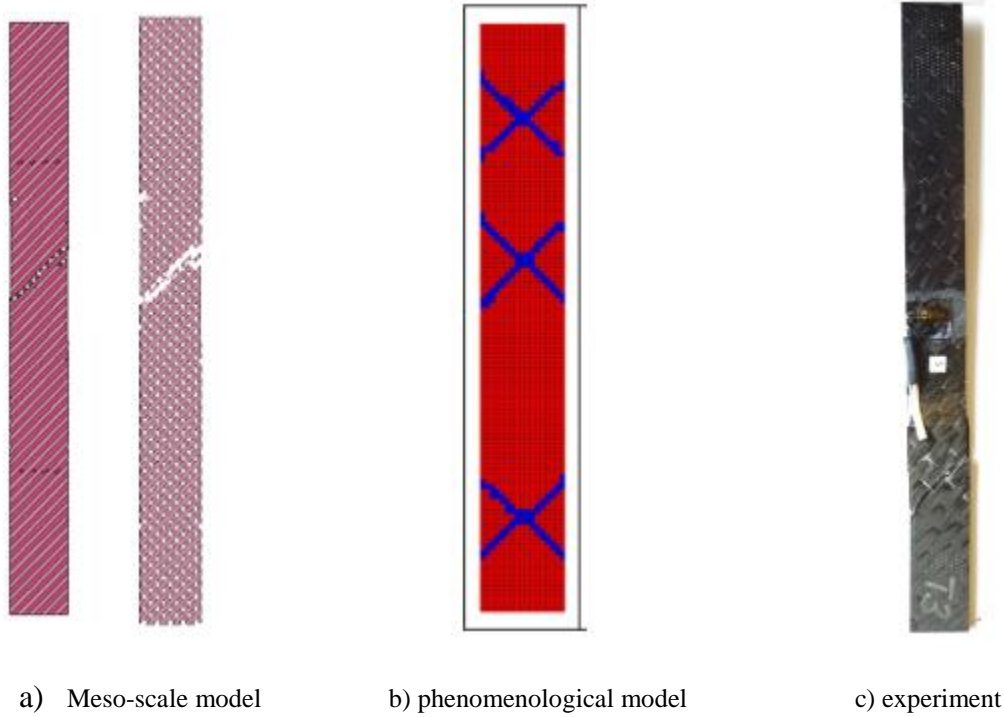


Figure 9: Crack Paths in a [45/-45/-45/45] Laminate Coupon

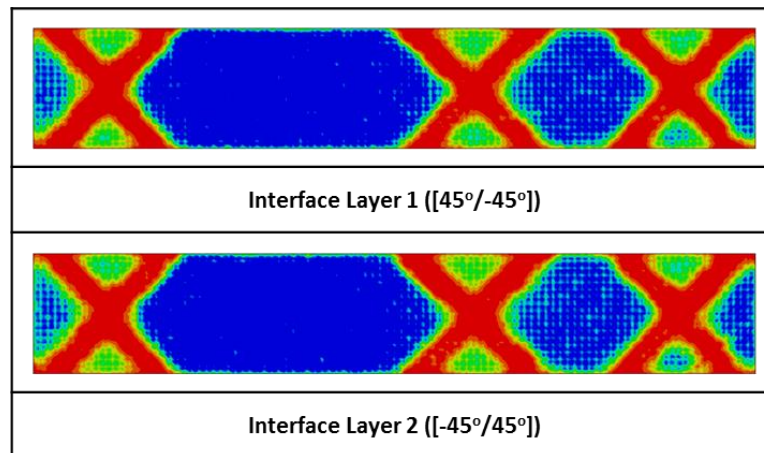


Figure 10: Delamination at Sub-laminate Interfaces in a [45/-45/-45/45] Laminate Coupon

Figure 9a shows the failure in the meso-scale model with matrix failure and fibers remaining intact. Figure 9b shows only the failure for phenomenological model. Figure 9c shows failure in the test coupon. There was excellent correlation for predicting cracking in the meso-scale model and phenomenological model as compared to the experiment.

Tensile loading 30 deg. angle ply:

In figure 11 the load versus axial strain results for a [30/-30/-30/30] laminate in tension are presented. One can see a good correlations of failure load and slope of the curve when comparing the simulation and the experimental results for both phenomenological and meso-scale models.

Failure paths in sub-laminate layers from the meso-scale model, the phenomenological model and the test coupon are presented in figure 12. Delamination at the interfaces from the phenomenological model are presented in figure 13. The sub-laminate layers fail mainly in the matrix, due to the in-plane shear stress reaching the failure limit. In fact the inter-laminar shear stress reaches the failure limit ahead of the in-plane shear stress which triggers delamination at the sub-laminate interfaces and ultimately causes the in-plane shear stress in the sub-laminate layers to reach the failure limit. In figure 13, the red color indicates complete delamination and the blue color indicates no delamination at the interfaces.

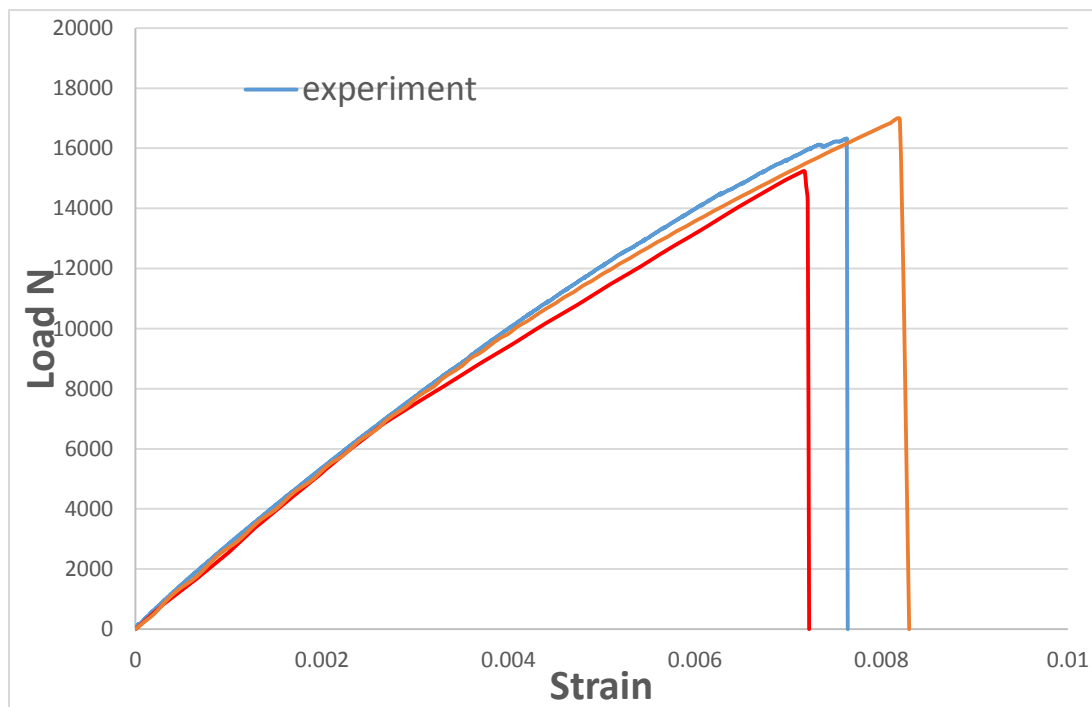


Figure 11: Load vs. Axial Strain in a [30/-30/-30/30] Laminate Coupon

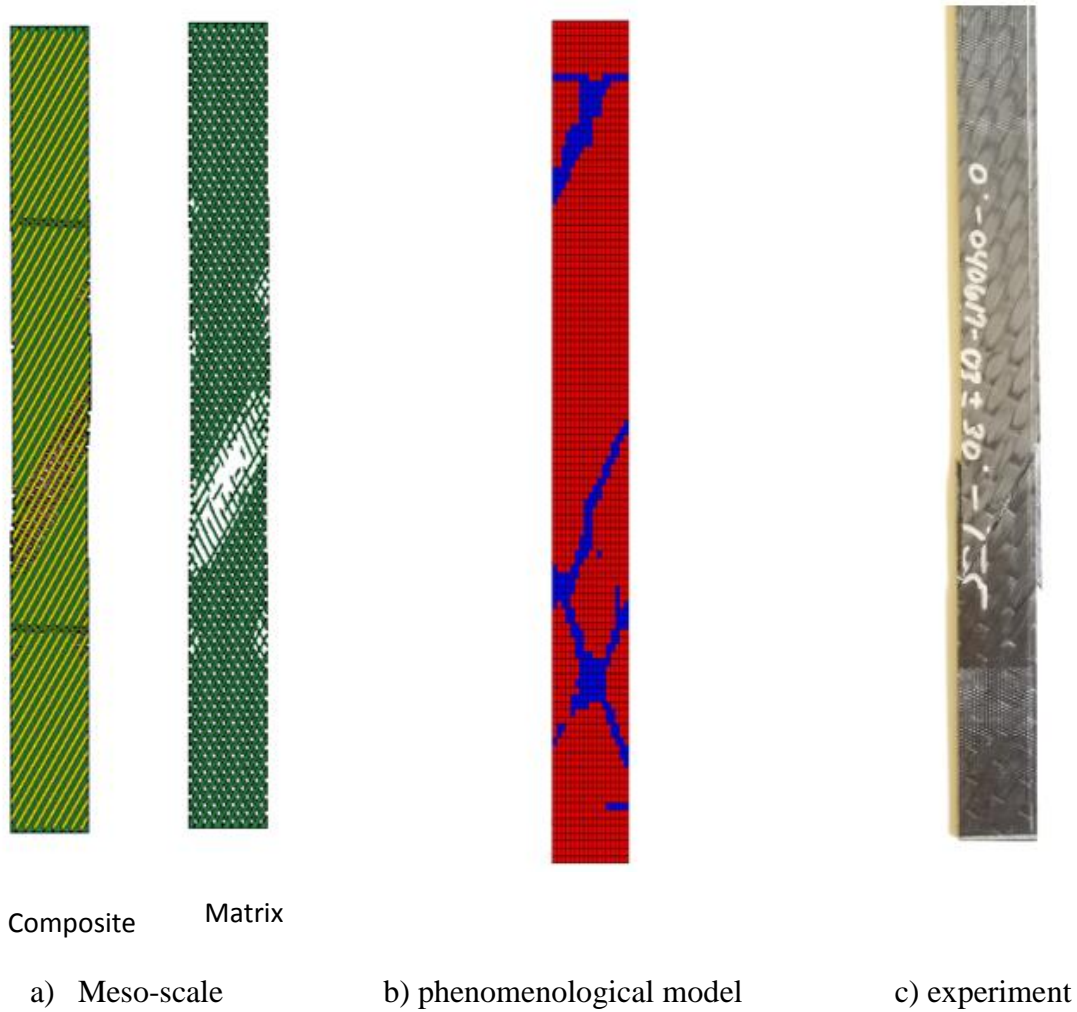


Figure 12: Crack Paths in a [30/-30/-30/30] Laminate Coupon

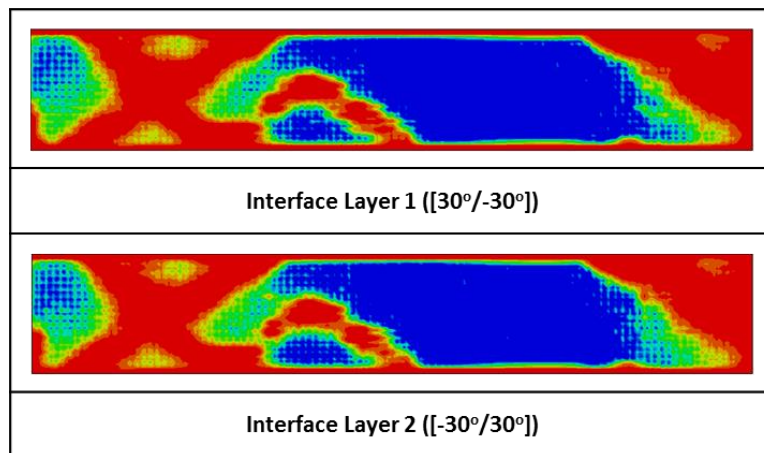


Figure 13: Delamination at Sub-laminate Interfaces in a [30/-30/-30/30] Laminate Coupon

Figure 12a shows the failure in the meso-scale model with matrix failing and fibers remaining intact. Figure 12b shows only the failure for phenomenological model. Figure 12c shows failure in the test coupon. There was excellent correlation in predicting cracking in the meso-scale model and the phenomenological model as compared to the experiment

Tensile loading 60 deg. angle ply:

In figure 14 the load versus axial strain results of a [60/-60/-60/60] laminate in tension are presented. One can see a good correlations of the failure load between the experimental result and the simulation from the phenomenological model and the meso-scale model. The slope of the curve obtained from the phenomenological model and meso-scale model correlates well with the test data for the most part except towards the end. It is evident from the test data that significant nonlinearity was present in the load strain curve. However the simulation could not capture the extent of nonlinearity and needs additional investigation regarding the coupling of in-plane shear strain and transverse strain.

Failure paths in sub-laminate layers obtained from the meso-scale model, the phenomenological model and the test coupon are presented in figure 15. The delaminations at interfaces obtained from the phenomenological model are presented in figure 16. The sub-laminate layers fail mainly in the matrix, due to the transverse stress reaching the failure limit. In fact the inter-laminar shear stresses lag the failure limits. The crack path is indicated by blue color in figure 15.

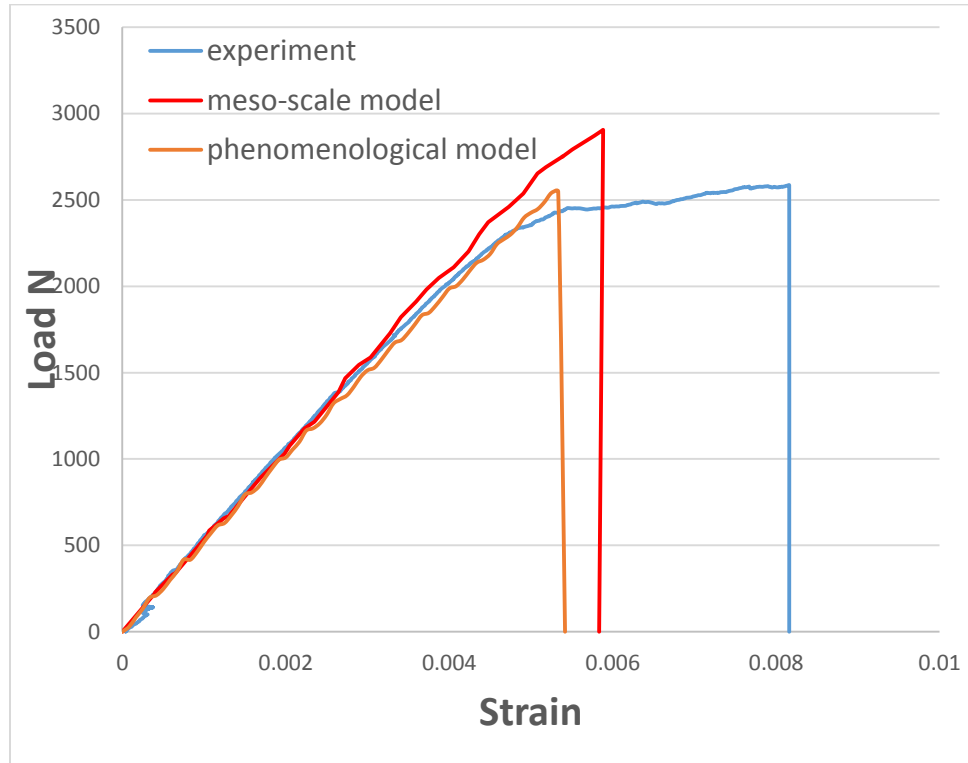


Figure 14: Load vs. Axial Strain in a [60/-60/-60/60] L

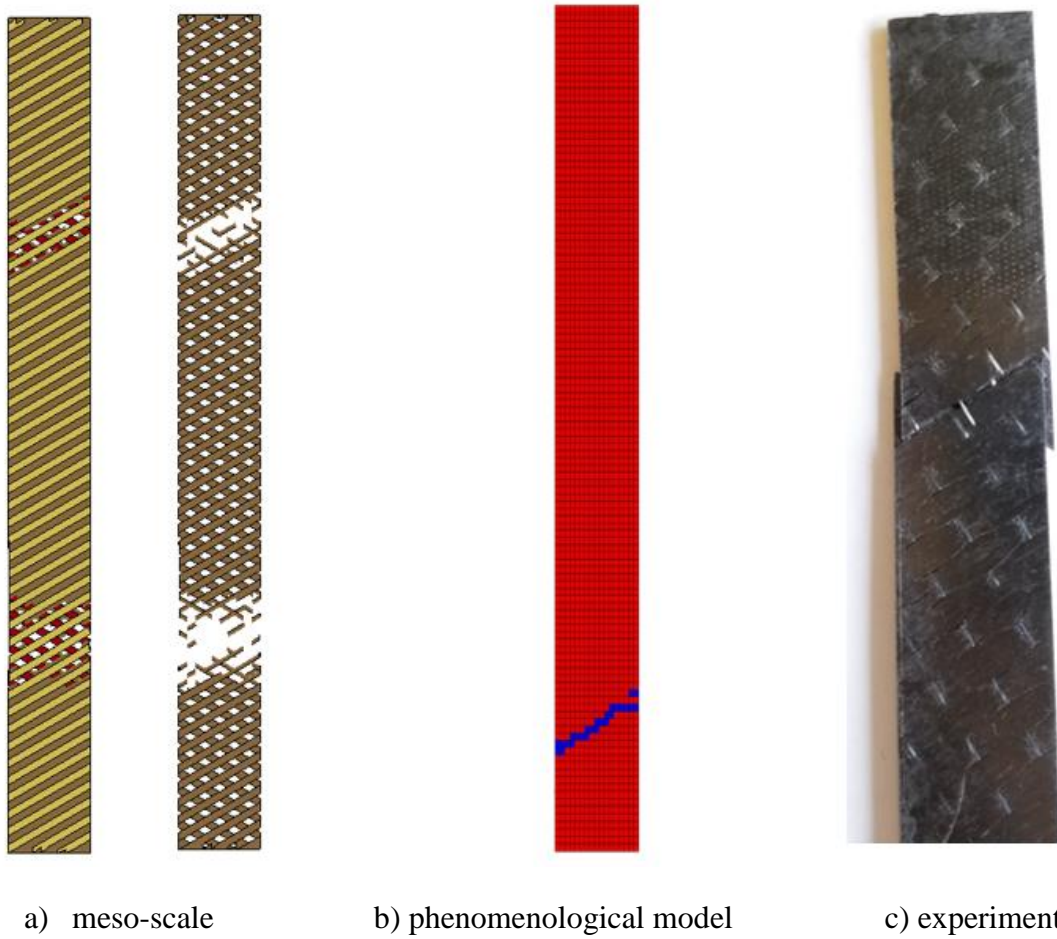


Figure 15: Crack Paths in a [60/-60/-60/60] Laminate Coupon

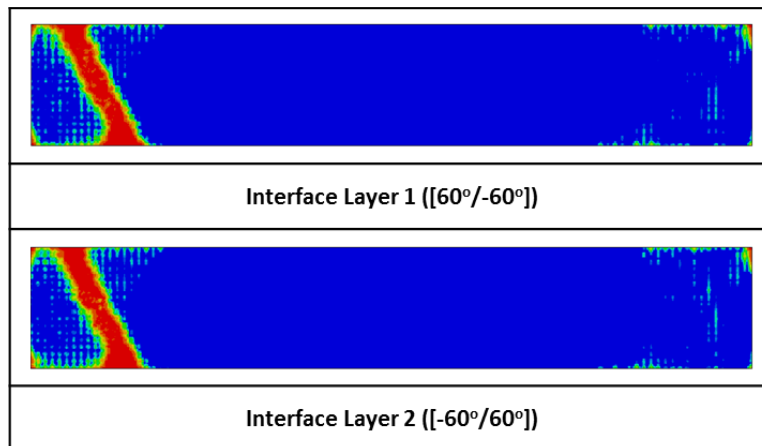


Figure16: Delamination at Sub-laminate Interfaces in a [60/-60/-60/60] Laminate Coupon

Figure 15a shows the failure in the meso-scale model with matrix failing and fibers remaining intact. Figure 15b shows only the failure for the phenomenological model. Figure 15c shows failure in the test coupon. There was excellent correlation for predicting cracking in the meso-scale model and the phenomenological model as compared to the experiment

In figure 16, delamination contour plots at the sub-laminate interfaces are presented for phenomenological model. Red indicates complete delamination and indicates no delamination at the interfaces. One can observe that the delamination is confined to the crack path in the sub-laminate layers which indicates that the delamination occurs due to in-plane damage and is not triggered by inter-laminar shear stresses as noticed in a [30/-30/-30/30] laminate.

Conclusions:

A meso-scale and a phenomenological model for progressive failure analysis of off-axis composite laminates was developed and numerical predictions were compared with experimental results. The meso-scale models involve modeling the tow and resin regions explicitly. The tows in the composite are modeled with an orthotropic material with Chang-Chang failure criteria. The resin regions are modeled using an elastic-plastic material model. The inter-layer damage was modeled using a cohesive zone. The phenomenological damage model previously developed by the authors was improved in the present study to simulate the shear behavior more accurately. Both the meso-scale and phenomenological models were first calibrated against the (45/-45/45/-45) degree lay-up and subsequently validated against the other off-axis layups. For the (30/-30/-30/30) degree lay-up, prediction of the load versus strain and the crack path matched very closely with the experimental results. For the (60/-60/-60/60) lay-up, phenomenological model and meso-scale models were not able to capture the nonlinearity as observed in the experiment but showed excellent correlation for the load and stiffness. The crack path predicted from both the models matched with experimental results very closely. It shall also be noted that the ability of the models to predict crack propagation parallel to the fiber orientations was due to the enhanced shear stress degradation model. Prior study with the instantaneous shear degradation model did not predict crack trajectories nearly as well when the element edges were aligned with the global axes.

References:

1. Hashin, Z., and Rotem. A., “A fatigue failure criterion for fiber reinforcement materials”, Journal of Composite Materials, Vol 7, 1973, pp 448-464.
2. Hashin, Z. “Failure criteria for unidirectional fiber composites”, Journal of Applied Mechanics, Vol 47, 1980, pp 329-334.
3. Davila, C.G., Camanho, P.P., and Rose, C.A., “Failure criteria for FRP laminates”, Journal of composite materials”, Vol 39, No. 4, 2005, pp 323-345.
4. Pinho, S.T., Davila, C.G., Camanho, P.P., Iannucci, L., and Robinson, P., “Failure models and criteria for FRP under in-plane or three-dimensional stress states including shear non-linearity, NASA TM-213530, NASA Langley Research Center, Hampton, VA 23681, Feb 2005.
5. Phillips, E., Herakovich, C., Graham, L., “Damage development in composites with large stress gradients”, Composite Science and Technology, Vol 61, 2001, pp 2169-2182.
6. Hirsekorn, H, Fagiano, C., Doitrand, A., Lapeyronnie, P., Chiaruttini, V., “Meso-scale modeling of damage in textile composites with compared and nested reinforcements”, ECCM16- 16th European Conference on Composite Materials”, June 22-26, Spain, 2014.
7. Arunkumar Satyanarayana and Philip Bogert, “Influence of Shear Stiffness Degradation on Crack paths in Uni-directional Composite Laminates”, NASA/TM-2017-00000 in Review process.
8. Satyanarayana, A., Bogert, P., Karayev, Z. K., Nordman, S. P., Hamid, “Influence of Finite Element Size in Residual Strength Prediction of Composite Structures,” Proceedings of the 53rd AIAA/ASME/ASCE/AHS/ASC Structures, Structural Dynamics and Materials Conference, Honolulu, Hawaii, April 2012, AIAA-2012-1619.
9. Song, K., Li, Y., and Rose, C. A., “Continuum Damage Mechanics Models for the Analysis of Progressive Failure in Open-Hole Tension Laminates,” Proceedings of the 52nd AIAA/ASME/ASCE/AHS/ASC Structures, Structural Dynamics and Materials Conference, Denver, Colorado, April 2011, AIAA-2011-1861.